

# **MedCLIVAR Exchange Grants Report**

June 2011

## **Mid-Holocene relative sea-level change in the Gulf of Gabès (southern Tunisia)**

Applicant:  
**Gabriella Ruggieri**

*Dipartimento di Scienze di Base  
Università of Urbino  
(IT).*

Host Institution:  
**Barbara Mauz**

*School of Environmental  
Sciences, University of Liverpool  
(UK)*

## **1. PURPOSE OF THE VISIT**

The purpose of the visit was to conduct petrographic and cathodoluminescence analysis on samples of mid-Holocene deposits originating from the coast of the Gulf of Gabès (Tunisia). Since the 1980<sup>th</sup> these deposits were studied by several workers due their potential indicative meaning for a mid-Holocene palaeo- shorelines higher than today (Paskoff and Sanlaville, 1983; Jedoui et al., 1998; Morhange and Pirazzoli, 2005). The analysis should allow obtaining more information about the change of the relative sea-level in the Gulf since the mid-Holocene.

The research visit was hosted by the School of Environmental Sciences, University of Liverpool (UK).

## **2. WORK CARRIED OUT DURING THE VISIT**

A detailed study on the microfacies analysis and diagenetic settings of the mid-Holocene beachrock deposit of Gabès Gulf was conducted.

In particular I analysed nine impregnated and polished thin sections using petrographic and cathodoluminescence analyses. While the first method allows describing composition, texture and matrix, the second allows identifying diagenetic phases and stages of cementation. During the first week, the Nikon Eclipse 6400POL petrographic microscope was used to describe and classify the samples following Dunham (1962), Folk (1962), Krumbein and Sloss (1963), Zuffa (1979) and Tucker (1981). Relative abundances of skeletal grains, non-skeletal grains, mud, and diagenetic components (porosity, cement) were determined for each thin section through a qualitative method. The work in the second week focused on studying the carbonate cement. Cathodoluminescence analysis was conducted using a Technosyn 8200 Mk operating at 10 kV and 30-40 mA with an unfocused electron beam under He atmosphere at 0.2 Torr vacuum pressure.

The results of the analyses were elaborated during the last weeks of my stay in order to establish a vertical microfacies succession using criteria from lithology, sedimentary structures, texture, frequency and composition of allochems according to Flugel (2004). The depositional environmental as well as the diagenetic setting and evolution environment were also determined using these data.

### 3. RESULTS

Based on the approach described above I identified four microfacies which I call EGa, EGb, EGc, EGd (Fig.1).

*EGa (samples eg2, eg3, eg6, eg7, Fig. 1):*

Sandy grainstone, moderately sorted, dominant components are ooids (64%) and skeletal grains (30%). The ooids are superficial and normal ooids showing one or more concentric layers as coating around the nucleus which exhibit a tangential orientation of aragonite crystal. The nucleus is dominantly bio- or siliciclastic grain. The skeletal grains are constituted by red algae (Halimeda, Melobesiae), foraminifera (Miliolidi and Elphidium) and mollusc shell remains (bivalves, echinoderm and gasteropodes). The primary porosity is quite obscured by cement. The cements include marine isopachous bladed high Magnesium calcite (HMC) cement, scalenohedral dogtooth cement, gravitational fabric calcite cement, interparticle bridge of microcrystalline or granular calcite cement.

*EGb (sample eg4, Fig. 1.):*

Sandy grainstone, moderately to poorly sorted, part of the grains is aligned in a preferred grain orientation, dominant components are ooids (57%), bivalve shells (10 %) and sub-angular siliciclastic grains (5 %). Most ooids are superficial ooids and present a circular shape with tangential fabric of carbonate crystals. The nucleus is bioclast or siliciclastic grain. The bivalve shell exhibit elongate shape (most of them are conus cerithes) favouring fabric orientation. Others skeletal grains are: foraminifera (Miliolidi), coralline red algae (Halimeda, Melobesiae), echinoderma. The cement occurs as an irregular rim around the grains with bladed or radiaxial fibrous type cement with gravitational fabric. The major thickness of cement occurs as gravitational fabric in the intergranular space.

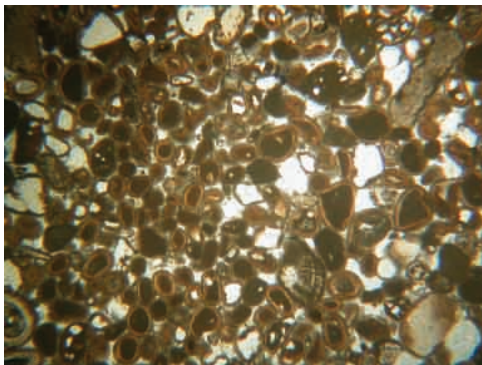
*EGc (samples eg1, eg5, Fig. 1):*

Litharenite bearing carbonate detrital components, well-sorted, composition is dominated by non-skeletal grains (95%) which are ooids and siliciclastic grains. The ooids are superficial in structure with concentric layers showing relics of original tangential fabric due to micritisation. The coating shows ruptures indicating a reworked origin of the ooids. Quartz and feldspars with sub-angular shape are the dominant constituents of the siliciclastic component. Few foraminifera and echinoderma are present exhibiting recrystallised shells filled with micrite. The cement displays a coarsely crystalline rim of

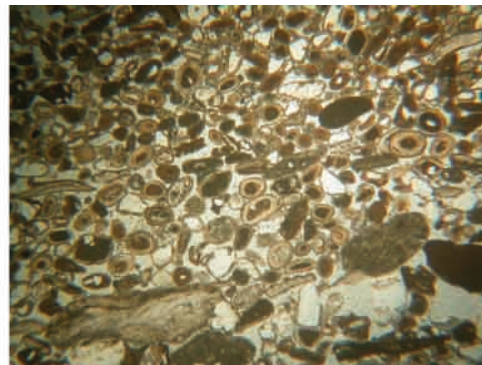
dogtooth type cement with irregular thickness and circumgranular calcite that fills almost all the voids.

*EGd (eg8 sample, Fig. 1):*

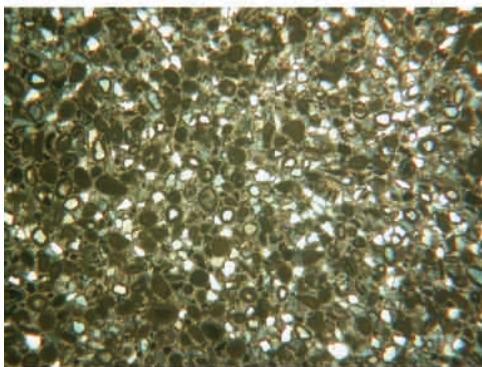
Coarse bioclastic sand, very poorly sorted and poorly cemented. Coralline red algae (10%) (*Melobesiae*, *Halimeda*), foraminifera (20%) (*Miliolidi*, *Ammonia*) and shell fragments (10%) of gastropods and bivalve are abundant. Coarse sand lithoclasts (30%) dominate the non-skeletal grain fraction. The cement is almost absent: a very thin rim of microcrystal calcite around the grains.



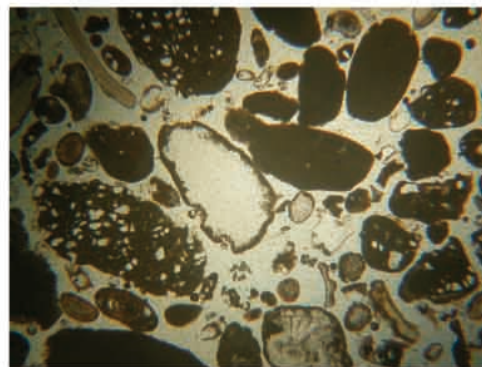
Microfacies EGa



Microfacies EGb



Microfacies EGc



Microfacies EGd

Fig. 1: Thin sections showing fabric, texture and compositions of microfacies at normal lighth. For more detail

### 3.1. Calcite Cements

The beachrock samples under examination show various diagenetic features, fabrics and texture. From the petrographic analysis it was hypothesised that High-Mg calcite and (low-Mg) calcite is the dominant carbonate cement. High-Mg calcite occurs as isopachous bladed rim cements, micritic neomorphic cements and microsparite. Calcite occurs as scalenohedral dogtooth, microsparite and circum-granular cement. Figure 2 shows the different colours of cement under cathodoluminescence analysis.

#### *Isopachous microcrystalline rim (Fig. 2)*

Isopachous microcrystalline fabric forms a rim around the grains. The shape of this cement is bladed in EG6 and eg7 (size < 25  $\mu\text{m}$ ) and dogtooth within eg2, eg3, eg4 (size <10  $\mu\text{m}$ ). Under cathodoluminescence (CL), the isopachous rim cements emitted a very dull blue colour.

#### *Scalenohedral dogtooth (Fig. 2)*

Scalenohedral dogtooth crystals with irregular and broken rim occur around grains. Moreover, the crystals are also observed on isopachous microcrystalline rim cement with crystal axes parallel to the growth direction of the rim cement or on very thin rim cement. The size of dogtooth crystals is about 1 mm where they form a meniscus or gravitational fabric cement (EG4, EG7). Under CL the dogtooth cement exhibits a dull blue colour with an outer margin of bright luminescent CL.

#### *Microsparite Fig. 2)*

Microsparite cements fill most of the inter-particles primary porosity with bridge fabric cement. Under CL it exhibits a non-luminescent or blue colour. Biotic voids are filled by microsparite showing bright yellow-orange bands.

#### *Micrite (Fig. 2)*

Pellets, ooids and shell remains experience neomorphic transformation to micrite. Under CL this micrite exhibits a variable colour as a function of its elemental composition. If the micrite is a diagenetic product of red algae, the CL colour is red or violet/red. If the micrite is a diagenetic result of ooids, its CL colour is violet. When shell remains are micritised, the CL is red or yellow-orange.

#### *Circum-granular (Fig. 2)*

Circum-granular calcite fills almost completely the voids in EG1 and EG5. Under CL it exhibits a blue colour with an outer band of bright CL colour.

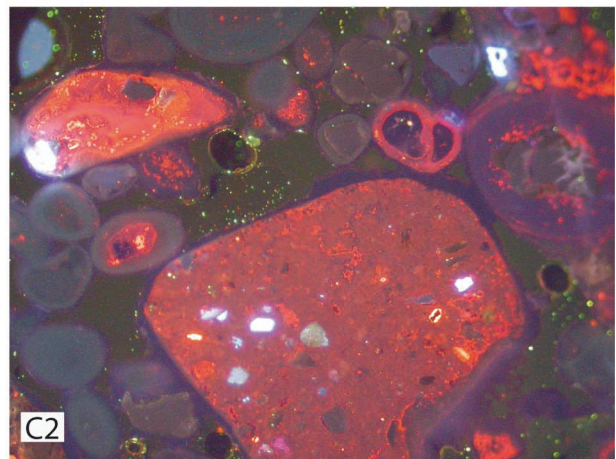
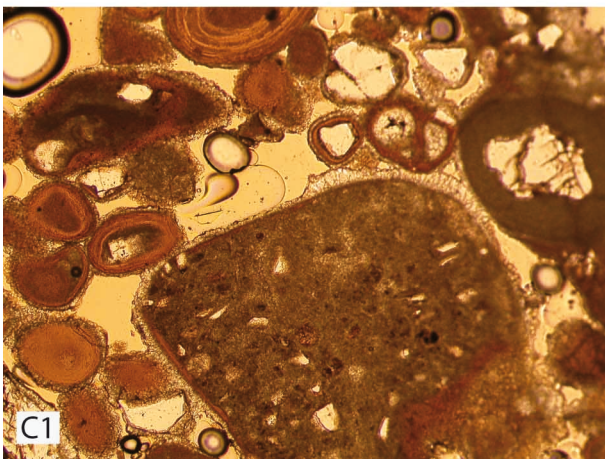
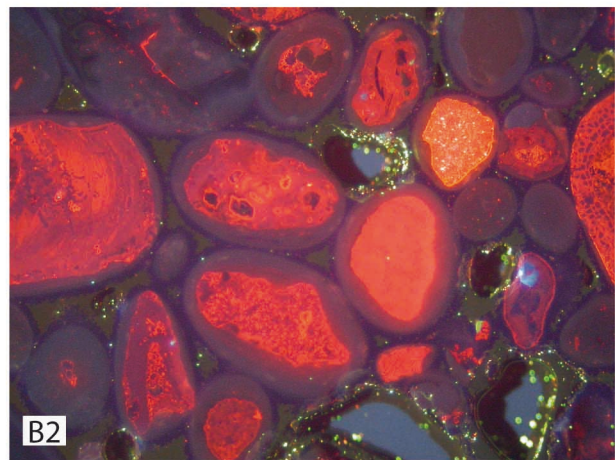
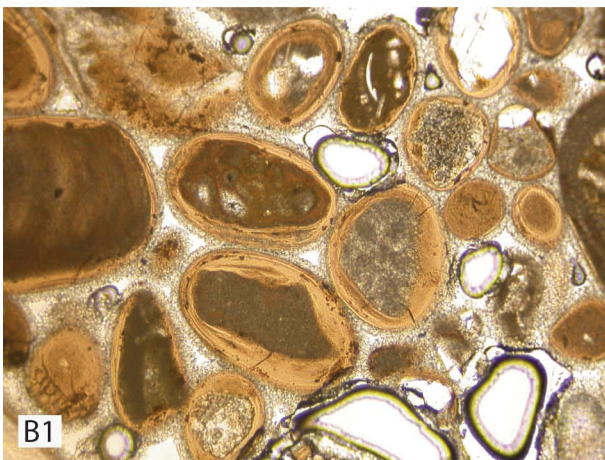
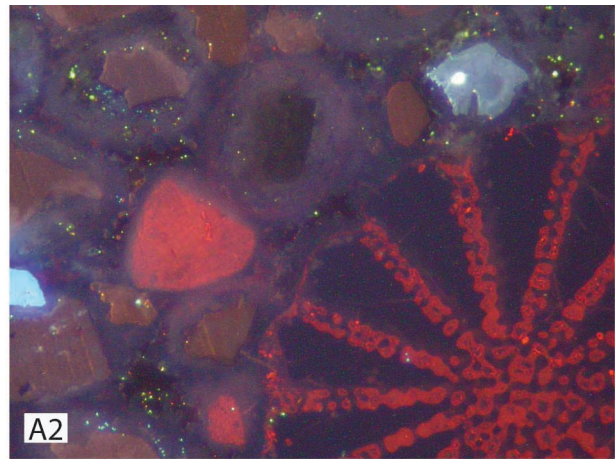
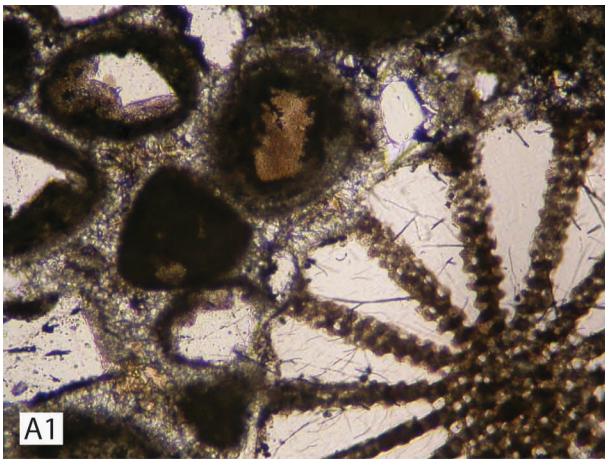


Fig. 2: Thin sections images from transmitting light (A1, B1, C1) and cathode luminescence (A2, B2, C2). Note the violet cortex and scalenoedral dogtooth cement in A2; a very dull blue isopachous rim cements in B2 and C2. Finally in the medium north eastern borders of C1 image the lithoclast exhibits a dogtooth cements with gravitation fabrics closed to micritized ooid. Under cathodluminescents effect the cement exhibits a very dull blue CL colour with a thin layer of bright red colour in the outermost part of it.

### **3.2. Interpretation of Diagenetic setting**

The EGa, EGb microfacies, exhibit the typical characteristics associated with marine phreatic diagenesis: isopachous microcrystalline fabric. CL shows that this cement is characterized by very dull blue or violet cement. This colour is described by Aimieux (1989) to be the intrinsic colour of carbonate. The faint Mn as CL activator and the isopachous fabric indicate precipitation from oxidising water under shallow marine condition. Moreover, qualitative petrographic analysis shows that the cement is relatively rich in Mg. The high-Mg calcite composition of the cement suggests a significant influence of sea-water in their precipitation (Flügel et al., 2004). Non luminescent (violet) scalenohedral cement differs from circum-granular isopachous rim cement in crystal shape and size indicating precipitation under conditions of reduced sea-water agitation and reduced availability of  $Mg^{2+}$  ions. Moreover, the outer margin of dogtooth crystals exhibiting bright luminescent CL is generally interpreted as being caused by a decrease in redox potential (Eh) which results in reduction of  $Mn^{4+}$  to  $Mn^{2+}$  where  $Mn^{2+}$  goes into solution and is subsequently incorporated in calcite lattice. Decreasing Eh is expected to occur alongside progressive marine burial diagenesis (Kaufmann, 2007), or in a stagnant marine phreatic zone at near-surface temperature and pressure conditions interpreted as a sign of fresh-water flooding by Aimieux (1989). The growth of dogtooth crystals starts on the surface of components or syntaxially on isopachous rim.

The growth of dogtooth crystals on very thin rim cement probably indicates partial neomorphism replacement of bladed isopachous rim cement.

The pore filling proceeds toward the central area of the pore through circum-granular fabric calcite cement.

Both types of cement are interpreted to reflect a progressive shift from marine to meteoric diagenesis environment. The corrosion surface of bladed rim cement, the neomorphic replacement with dogtooth cement and the irregular rim with meniscus and gravitational fabric are evidence for fresh water influence during the early diagenesis.

### **3.3 Interpretation of Microfacies**

The petrographic and textural analysis of thin sections indicate that the microfacies were part of a shallow marine environment between subtidal and supratidal environment.

Microfacies Ega and Egb exhibit a vertical shallowing upward succession.

EGa: The absence of sedimentary structure within the sand sized microfacies Ega suggests a massive deposition or a reworking of sediment by biotic components. This could be interpreted as deposit of low energy sub-tidal or deeper intertidal environment.

EGb: Within the microfacies Egb the shell orientation are typical of the intertidal environment because of transported shell by sea water during low and high tide. This feature could be associated with a persistent laminar sea current of the intertidal environment. The isopachous rim fabric and HMC composition of cement support the idea about a marine zone within the marine-phreatic diagenetic environment.

EGc: The micritisation of the ooids's cortex within EGc suggests that the ooids are not of autochthonous origin. Neomorphic replacement of aragonite by calcite is the first diagenetic phase occurring in the microfacies Egc.. Moreover, the smaller grain size and the well sorting of grain testify sustained water agitation. However, the well sorting could be inherited in which case the sorting cannot be associated with the energy of the sea water. The EGc is characterised by enrichment of the siliciclastic component. The possible explanation for this major shift in composition is an influx of terrigenous sediment from a proximal river caused by a seaward shift of the shoreline due to lowering of the relative sea level. In this case microfacies (Ega, Egb) would correspond to sea-level highstand and the Egc would record a transition toward the fall in sea level.

More information about the environmental setting of the microfacies is obtained from the cement: arrangement and fabrics of dog-tooth cement indicating meteoric environment is common within EGc, Egb and Ega suggesting a seaward shift of the shoreline due to sea-level fall. Moreover, the range of CL colour exhibited by dog tooth cement from blue to red, emphasises the transition from marine phreatic to meteoric diagenetic processes.

Finally the EGd microfacies represent the supratidal deposits still today under formation.



Fig.2: Thin sections images from transmitting light (A1, B1, C1) and cathodoluminescence (A2, B2, C2). Note the violet cortex and scalenohedral dogtooth cement in A2; a very dull blue isopachous rim cements in B2 and C2. Finally in the medium north eastern borders of C1 image the lithoclast exhibits a dogtooth cements with gravitation fabrics closed to micritized ooid. Under cathodoluminescents effect the cement exhibits a very dull blue CL colour with a thin layer of bright red colour in the outermost part of it.

#### **4. FUTURE COLLABORATION**

In this four weeks work, the petrographic and cathodoluminescent analysis allows us to obtain more information about the mid Holocene paleoenvironments at Gulf of Gabès. However more others investigations need to be make with the aim to confirm a firstly interpretation. The next collaboration will cover RXD and OSL dating.

#### **5. PROJECTED PUBLICATIONS**

The material and the results obtained during the Medclivar Exchange grant in Liverpool University will be used and submitted for a future publication:

- Ruggieri G., Mauz B. Emelgiab N., Spada G., Mid-Holocene shoreline progradation in the Gabès Gulf, southeastern tunisia. *Marine Geology*.

#### **6. REFERENCES**

Amieux P., Bernier P., Dalongeville R, Medwecki V. (1989), Cathodoluminescence of carbonate-cemented Holocene beachrock from the Togo coastline (West Africa): an approach to early diagenesis. *Sedimentary Heology*, 65, 261-272.

Dunham R. J. (1962), Classification of carbonate rocks according to depositional texture. In: *Classification of Carbonate Rock*; Ed. By W. E. Ham. Mem. Am. Ass. Petrol. Geol. 1, 108-121.

Folk R. L. (1962), Spectral subdivision of limeston types. In: *Classification of Carbonate Rock*; Ed. By W. E. Ham. Mem. Am. Ass. Petrol. Geol. 1, 62-84.

Flugel E. (2004), *Microfacies of Carbonate Rocks*. Springer, Stutz, Wurzburg, 976 pp.

Jedoui, Y., Kallel, N., Fontugne, M., Ben Ismail, H., M Rabet, A., Montacer, M. (1998), A high relative sea-level stand in the middle Holocene of south-eastern Tunisia. *Marine Geology*, 147, 123-130.

Kaufmann B., (2007), Diagenesis of Middle Devonian Carbonate Mounds of the Mader Basin (eastern AntiAtlas, Marocco). *Journal of Sedimentary Research*, vol 67,5, 945-956.

Krumbein W. C. and Sloss L.L (1951), *Stratigraphy and Sedimentation*. San Francisco, W. H. Freeman and Co., 497pp.

Morhange, C. and Pirazzoli P.A. (2005), Mid-Holocene emergence of southern Tunisian coasts. *Marine Geology*, 220, 205-213.

Paskoff, R. and P. Sanlaville (1983), *Les Cotes de la Tunisie. Variations du Niveau Marin depuis le Tyrrhénien* (Maison de l'Orient Meditteraneen, Lyon), pp.192.

Strasser D., Davoud E., Jedoui Y. (1988), Carbonate Cements in Holocene beacrock: example from Bairet El Biban southeastern Tunisia, *Sedimentary Geology*, 62 , 89-100.

Tucker M. E. (1981), *Sedimentary petrology: an Introduction*. Pp252. Blackwells, Oxford.

Vousdoukas, M. I., Velegrakis A. F., Plomaritis T. A. (2007), Beachrock occurrence, characteristics, formation mechanisms and impacts. *Earth Science Review*, 85, 23-46.

Zuffa G. G. (1979), Hybrid arenites: their composition and classification. *J. Sed. Petrology*, 50, 21-29.